Article

Electrospinning as a New Technique To Control the Crystal Morphology and Molecular Orientation of Polyoxymethylene Nanofibers

Thontree Kongkhlang, Kohji Tashiro, Masaya Kotaki, and Suwabun Chirachanchai

J. Am. Chem. Soc., **2008**, 130 (46), 15460-15466 • DOI: 10.1021/ja804185s • Publication Date (Web): 25 October 2008

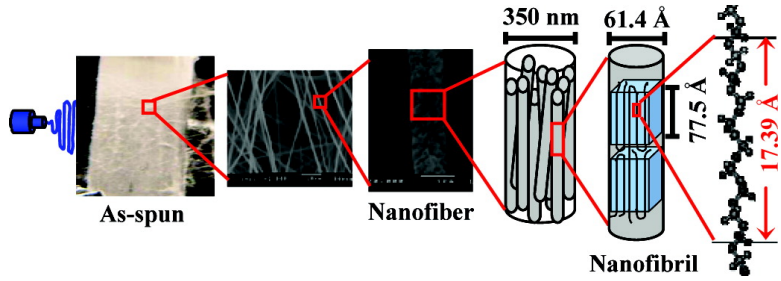

More About This Article

Additional resources and features associated with this article are available within the HTML version:

- Supporting Information
- Access to high resolution figures
- Links to articles and content related to this article
- Copyright permission to reproduce figures and/or text from this article

View the Full Text HTML

J|A|C|S
ARTICLES

Published on Web 10/25/2008

Electrospinning as a New Technique To Control the Crystal Morphology and Molecular Orientation of Polyoxymethylene Nanofibers

Thontree Kongkhlang,[†] Kohji Tashiro,[‡] Masaya Kotaki,[§] and Suwabun Chirachanchai*,[†]

The Petroleum and Petrochemical College, Chulalongkorn University, Chula Soi 12, Phyathai Road, Pathumwan, Bangkok, Thailand 10330, Department of Future Industry-oriented Basic Science and Materials, Graduate School of Engineering, Toyota Technological Institute, Tempaku, Nagoya 468-8511, Japan, and Department of Advanced Fibro-science, Kyoto Institute of Technology, Matsugasaki, Sakyo-ku, Kyoto 606-8585, Japan

Received June 9, 2008; E-mail: csuwabun@chula.ac.th

Abstract: Electrospinning is widely accepted as a simple and versatile technique for producing nanofibers. The present work, however, introduces a new concept of the electrospinning method for controlling the crystal morphology and molecular orientation of the nanofibers through an illustration of a case study of polyoxymethylene (POM) nanofibers. Isotropic and anisotropic electrospun POM nanofibers are successfully prepared by using a stationary collector and a rotating disk collector. By controlling the voltage and the take-up velocity of the disk rotator, the morphology changes between an extended chain crystal (ECC) and a folded chain crystal (FCC) as clarified by a detailed analysis of the X-ray diffraction and polarized infrared spectra of the POM nanofibers. Herman's orientation function and dichroic ratio lead us to a schematic conclusion—that (i) molecular orientation is parallel to the fiber axis in both isotropic and anisotropic POM nanofibers, (ii) a single nanofiber consists of a nanofibril assembly with a size of 60−70 Å and tilting at a certain degree, and (iii) the higher the take-up velocity, the smaller the nanofibril under the (9/5) helical structure of the POM chains. It should be emphasized here that the electrospinning method is no longer a single nanofiber producer but that it can be applied as a new instrument to control the morphology and chain orientation characteristics of polymer materials, opening a new research field in polymer science where we can understand the relationship between structure at the molecular level and the properties and performance at the macroscopic level.

Introduction

Up to now, electrospinning has been accepted as an efficient technique for the production of polymer fibers, with diameters ranging from nano- to microscale, providing high surface area-to-volume ratios, and it is of considerable interest for many applications, such as nanoparticle carriers in controlled release,[1] scaffolds in tissue engineering,[2] wound dressings,[3] military wear with chemical and biological toxin-resistance,[4,5] nanofibrous membranes or filters,[6] and electronic sensors.[7,8] The electrospinning process involves the application of a strong electrostatic field to initiate a polymer jet with a sharp decrease of the jet diameter after its formation.[9] A branching of the jet occurring during the electrospinning process further leads to a decrease in diameter. A time resolution of approximately 0.0125 ms was reported based on the mechanism of the jet formation in electrospinning.[10]

The production of macroscopically aligned nanofibers by modifying the fiber collecting system to incorporate a rotating mandrel collector,[10] a copper wire drum,[11] a scanning tip,[12] or conductive plates containing an insulating gap[13] have been proposed so far. The production of uniaxially aligned nanofibers of which the anisotropic properties are important for use in microelectronics and in a variety of electrical, optical, mechanical, and biomedical applications has also been considered.

[†] Chulalongkorn University.
[‡] Toyota Technological Institute.
[§] Kyoto Institute of Technology.

(1) Zeng, J.; Aigner, A.; Czubayko, F.; Kissel, T.; Wendorff, J. H.; Greiner, A. *Biomacromolecules* **2005**, *6*, 1484–1488.
(2) Yang, F.; Murugan, R.; Wang, S.; Ramakrishna, S. *Biomaterials* **2005**, *26*, 2603–2610.
(3) Chen, J. P.; Chang, G. Y.; Chen, J. K. *Colloids Surf., A* **2008**, *313−314*, 183–188.
(4) Gibson, P. W.; Schreuder-Gibson, H. L.; Rivin, D. *AIChE J.* **1999**, *45*, 190–195.
(5) Gibson, P. W.; Schreuder-Gibson, H. L. US Army Soldier and Biological Chemical Command Technical Report Natick/TR-99/016L, 1999.
(6) Sawicka, K. M.; Gouma, P. *J. Nanopart. Res.* **2006**, *8*, 769–781.
(7) Wang, X.; Drew, C.; Lee, S. H.; Senecal, K. J.; Kumar, J.; Samuelson, L. A. *Nano Lett.* **2002**, *2*, 1273–1275.
(8) Wang, A.; Singh, H.; Hatton, T. A.; Rutledge, G. C. *Polymer* **2004**, *45*, 5505–5514.
(9) Doshi, J.; Reneker, D. H. *J. Electrost.* **1995**, *35*, 151–160.
(10) Teo, W. E.; Kotaki, M.; Mo, X. M.; Ramakrishna, S. *Nanotechnology* **2005**, *16*, 918–924.
(11) Katta, P.; Alessandro, M.; Ramsier, R. D.; Chase, G. G. *Nano Lett.* **2004**, *4*, 2215–2218.
(12) Kameoka, J.; Orth, R.; Yang, Y.; Czaplewski, D.; Mathers, R.; Coates, G. W.; Craighead, H. G. *Nanotechnology* **2003**, *14*, 1124–1129.
(13) Li, D.; Wang, Y.; Xia, Y. *Adv. Mater.* **2004**, *16*, 361–366.

10.1021/ja804185s CCC: $40.75

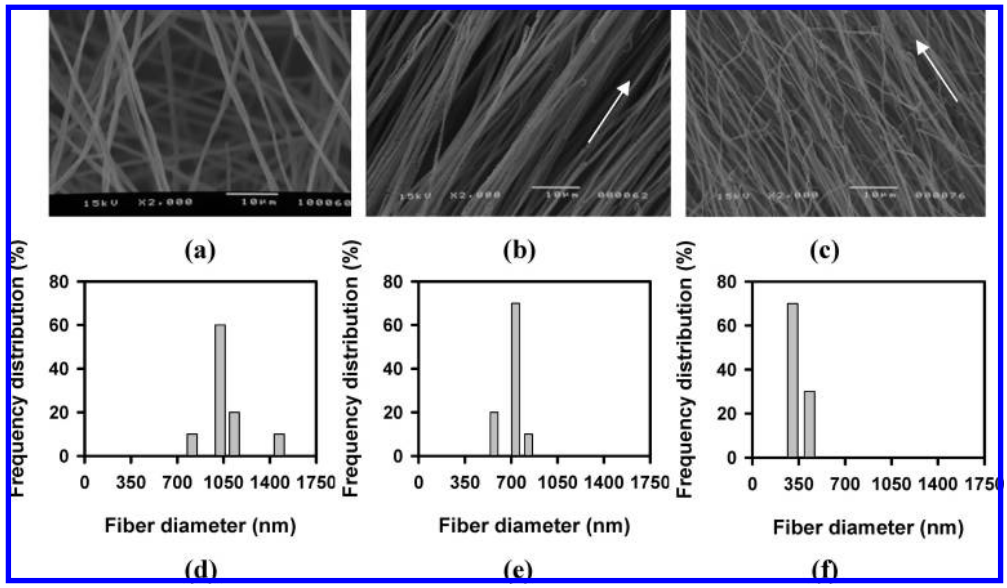

Figure 1. Scanning electron micrographs and frequency distribution of electrospun POM nanofiber obtained from using (a,d) a stationary collector, and using a rotating disk collector with a take-up velocity of (b, e) 630 m/min, and (c, f) 1890 m/min. Arrows indicate drawing direction.

Table 1. FTIR Band Assignment of Polyoxymethylene

mode	ECC[a]	FCC[a]	assignment[19]
$E_1(6)$, ⊥	1235, vs	1235, vs	CH_2 rock., δ(OCO), ν_s(COC)
$A_2(3)$, //	1097, vvs	1136, vvs	ν_a(COC), δ(OCO)
$E_1(7)$, ⊥	1092, vvs	1092, vvs	ν_a(COC)
$E_1(8)$, ⊥	935, vvs	935, vvs	ν_s(COC)
$A_2(4)$, //	897, vvs	1002, vvs	ν_a(COC), CH_2 rock.
$E_1(9)$, ⊥	628, s	630, s	δ(OCO)

[a] Relative intensity of the infrared band, s: strong, vs: very strong, vvs: very, very strong. [b] Raman-active and infrared-inactive $A_1(4)$ and $E_2(4)$ bands appear respectively at 919 and 1388 cm^{-1} for both FCC and ECC samples.

However, focused studies on the morphology and molecular orientation of polymer chains are very limited.[14,15]

Polyoxymethylene (POM), also known as polyacetal, is an important engineering thermoplastic as well as a crystalline polymer commonly used to replace metals and alloys due to its high tensile strength, impact resistance, stiffness, good dimensional stability, and corrosion resistance. The (9/5) helical structure was first proposed by Tadokoro et al. for the molecular conformation of POM to be hexagonal with unit cell parameters $a = 4.47$ Å and $c = 17.39$ Å.[16] Later, a more detailed (29/16) helical structure was proposed by Carazzolo from the layer line intervals.[17] Recently, Tashiro et al. has refined this crystal structure based on the synchrotron X-Ray and neutron diffraction data.[18] The crystal structure of the crystalline phase is generally classified into two types: a folded-chain or lamellar crystal (FCC) and an extended-chain crystal (ECC), depending on the crystallization conditions as well as on the thermal and mechanical histories.[19] Generally, the properties of POM are significantly influenced by the crystal morphology of the polymer. The typical FCC structure is achieved by crystallizing a dilute POM in a bromobenzene solution. This generates hexagon-shaped lamellar crystals with around 10 nm thickness, where the molecular chains are folded at the lamellar surface with the stems aligning normal to the surface.[20] The typical ECC structure is achieved through a heterogeneous cationic polymerization of trioxane, giving micron-sized needlelike single crystals where the extended POM molecules align parallel to the needle axis.[21,22] Drawing the fiber is another way to develop ECC-type POM.[19] The crystal morphology in the melt-grown bulk samples situates between the above two extremes.[23]

Melt-spun POM is an alternative choice for exploring new applications; however, there is difficulty in how to prepare POM melt under elevated temperature conditions without degradation.[24] In order to avoid this problem, the copolymer combined with a small amount of other comonomer is useful, as long as the crystallization behavior is not seriously affected.[25]

Recently, we succeeded in developing electrospun POM nanofibers, where we proved that inevitable nanopores are generated under thermally induced phase separation (TIPS) and vapor-induced phase separation (VIPS) mechanisms.[26] However, by controlling the spinning electrical voltage and rotating speed of the disk rotator, we found that (i) the electrospinning easily controls the crystal morphology, and (ii) the morphology is interchangeable. It is important to note that by detailed analysis, together with the controlled spinning conditions (especially the spinning voltage and the type of the fiber collector including its spinning velocity), we found that we not only produce an inevitable nanoporous nanofiber but are also controlling the

(14) Fennessey, S. F.; Farris, R. J. *Polymer* **2004**, *45*, 4217–4225.
(15) Kakade, M. V.; Givens, S.; Gardner, K.; Lee, K. H.; Chase, D. B.; Rabolt, J. F. *J. Am. Chem. Soc.* **2007**, *129*, 2777–2782.
(16) Tadokoro, H.; Yasumoto, S.; Murahashi, S.; Nitta, I. *J. Polym. Sci.* **1960**, *44*, 266–269.
(17) Carazzolo, G. *J. Polym. Sci., Part A* **1960**, *1*, 1573–1583.
(18) Tashiro, K.; Kamae, T.; Asanaga, H.; Oikawa, T. *Macromolecules* **2004**, *37*, 826–830.
(19) Kobayashi, M.; Sakashita, M. *J. Chem. Phys.* **1992**, *1*, 748–760.
(20) Bassett, D. C.; Dammont, F. R.; Salovey, R. *Polymer* **1964**, *5*, 579–588.
(21) Tadokoro, H.; Kobayashi, M.; Kawaguchi, Y.; Kobayashi, A.; Murahashi, S. *J. Chem. Phys.* **1963**, *38*, 703–721.
(22) Carter, D. R.; Baer, E. *J. Appl. Phys.* **1966**, *37*, 4060–4065.
(23) Hama, H.; Tashiro, K. *Polymer* **2003**, *44*, 3107–3116.
(24) Samon, J. M.; Schultz, J. M.; Hsiao, B. S.; Khot, S.; Johnson, H. R. *Polymer* **2001**, *42*, 1547–1559.
(25) Shimomura, M.; Iguchi, M.; Kobayashi, M. *Polymer* **1988**, *29*, 351–357.
(26) Kongkhlang, T.; Kotaki, M.; Umemura, T.; Kousaka, Y.; Nakaya, D.; Chirachanchai, S. *Macromolecules* **2008**, *41*, 4746–4752.

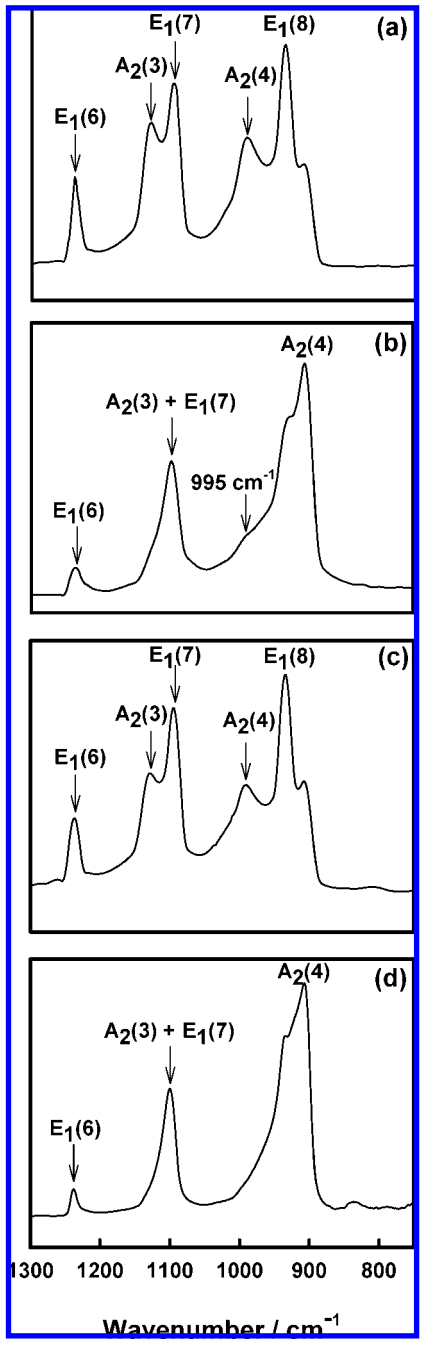

Figure 2. FTIR spectra of POM obtained from (a) cast film, (b) as-spun nanofiber, (c) recast film, and (d) respun nanofiber.

crystal morphology and molecular orientation at the molecular level. Therefore, we propose herein that electrospinning is no longer just a nanofiber preparation process, but it is a novel method to control the morphology and chain orientation. This makes it possible to investigate and understand how the physical and mechanical properties relate to the chain morphologies.

Generally, the morphologies of an extended chain crystal and of highly oriented fibers of polymer have been studied using various microscopy,[27] electron diffraction[18] and spectroscopy techniques.[19] The morphological information can be obtained by measuring the small-angle X-ray scattering (SAXS), but it is quite difficult to measure the SAXS pattern for a thin fiber using the X-ray diffraction on a laboratory level. Rather, an infrared spectral measurement is considered to be one of the best methods, in the case of POM, because the infrared spectra of POM are quite sensitive to the morphology, as shown by Kobayashi et al.[19] In this present study, we combine the polarized infrared spectra and the wide-angle X-ray diffraction for the various POM fibers produced by the electrospinning under the drawing equipment to determine the possibility of controlling the morphology of the electrospun fibers of POM. The present work, thus, shows a case study based on POM nanofiber about the application of a simple electrospinning technique to control the complicated morphology of polymer chain packing for the first time.

Results and Discussion

Figure 1 shows nanofibers with different diameters and morphologies when the rotating disk collector was applied. Due to the bending instability of the charged jet, randomly oriented nanofibers with a diameter of about 1000 nm was observed when the fiber was collected by a stationary collector (Figure 1a and 1d). On the other hand, aligned POM nanofibers were obtained by adjusting the take-up velocity of the rotating disk collector. Fiber alignment is significantly improved with the velocity (Figure 1b and 1c). As the take-up velocity increased from 630 m/min to 1890 m/min, the average diameter decreased from 700 to 350 nm (Figure 1e and 1f). This indicates that the fibers were stretched and aligned toward the rollup direction together with the control in fiber diameter via drawing. In order to understand how the electrospinning process, as well as the mechanical drawing, affects the crystal morphology and molecular orientation of the nanofiber, polarized FTIR and X-ray diffraction were utilized.

Crystal Morphology of Electrospun POM Nanofiber. Up to the present, various reports have shown how the vibrational spectrum of POM with different crystal morphologies exhibits specific spectral patterns, which can be used for the characterization of the morphological structure of the POM samples.[25,28−30] It should be noted that both ECC and FCC structures give the same X-ray diffraction pattern but remarkably different FTIR spectra.[25] The bands due to the A_2 symmetry species, having the transition dipole along the chain axis, show a significant high-frequency shift (as high as 100 cm^{-1}) in the FCC sample, as compared with those of the ECC sample (Table 1). On the other hand, the infrared- and Raman-active E_1 bands having the transition dipole perpendicular to the chain axis and the Raman-active and infrared-inactive A_1 and E_2 bands appear at the same frequencies in both the FCC and ECC samples.

The structure of the as-spun POM nanofibers was characterized by FTIR, and the result was compared with that acquired from a cast film (prepared from the same solution used for electrospinning). As evidenced in Figure 2b and Table 1, the as-spun POM nanofiber shows the characteristic IR peaks of $A_2(4)$, $E_1(8)$, $E_1(7)$, and $E_1(6)$ bands at the positions corresponding to the ECC morphology. A small shoulder at around 995 cm^{-1} is also observed, which is due to the amorphous phase in the system. The cast film, on the other hand, shows characteristic IR peaks in which the $A_2(4)$ band is located at 997 cm^{-1} and the $A_2(3)$ band is at 1130 cm^{-1}, corresponding to the band

(27) Snetivy, D.; Vancso, G. J. *Macromolecules* **1992**, *25*, 3320–3322.
(28) Shimomura, M.; Iguchi, M. *Polymer* **1982**, *23*, 509–513.
(29) Kobayashi, M.; Morishita, H.; Ishioka, T.; Iguchi, M.; Shimomura, M.; Ikeda, T. *J. Mol. Struct.* **1986**, *146*, 155.
(30) Morishita, H.; Kobayashi, M.; Komatsu, T. *Rep. Prog. Polym. Phys. Jpn.* **1987**, *30*, 127.

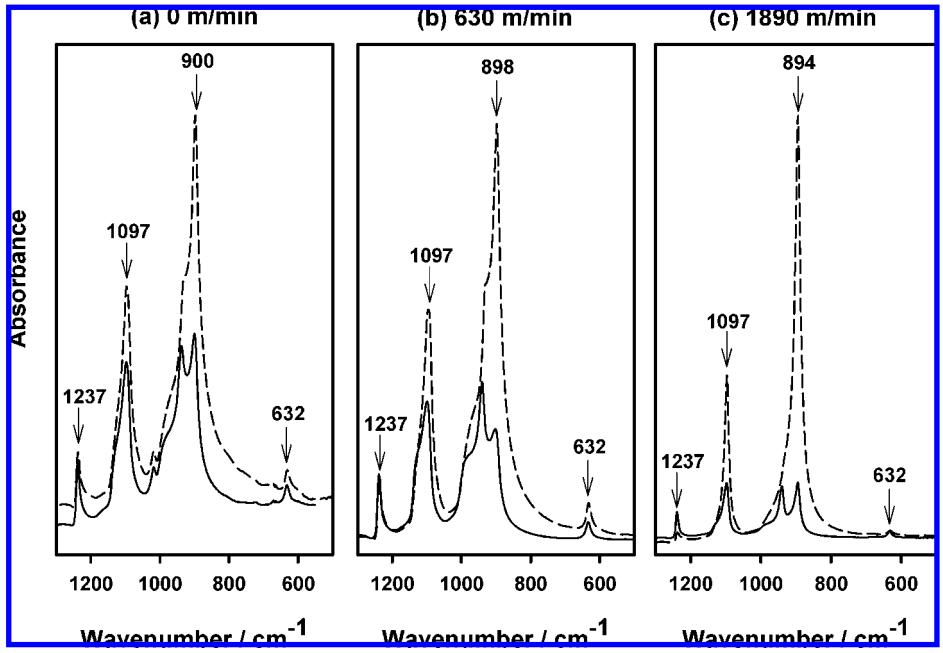

Figure 3. Polarized FTIR spectra of electrospun POM nanofiber from (a) a stationary collector and from a rotating disk collector at the velocity of (b) 630 m/min and (c) 1890 m/min. — Electric vector of an incident IR beam perpendicular to the fiber axis (⊥). - - - Electric vector of an incident IR beam parallel to the fiber axis (//).

Table 2. Dichroic Ratio ($A_{//}/A_{\perp}$) and Thermal Properties of POM Nanofibers at Various Rotating Disc Velocities

	linear velocity of rotating disk collector		
properties	0 (m/min)	630 (m/min)	1890 (m/min)
dichroic ratio (R) (A_2(3), ~1120 cm^{-1})	0.74	0.67	-
dichroic ratio (R) (A_2(4), ~900 cm^{-1})	2.15	3.95	7.87
ΔH_m, J/g (1st heating)	174	183	196
ΔH_m, J/g (2nd heating)	168	165	168

positions expected for the FCC morphology (Figure 2a). This implies that the crystal morphology is changed remarkably by the electrospinning process. Kobayashi and Sakashita reported that the ECC can be developed upon sample drawing.[19] For the electrospinning process, an electric force is required to overcome both surface tension and viscoelastic force for stretching the fiber. Taking this into consideration, the stretching during the electrospinning process is substantial for stretching the crystal region to get the ECC morphology.

To confirm that the electrospinning initiates the ECC chain morphology and that this packing can be easily changed to FCC, the as-spun POM nanofiber was dissolved in a hexafluoro-2-propanol (HFIP) solution followed by recasting and respinning. Figure 2c shows important information about the change from ECC to FCC after recasting. Moreover, the respun fiber shows that the ECC is recovered again after respinning (Figure 2d). This experimental result demonstrates clearly the effectiveness of controlling the ECC morphology via electrospinning. It should be emphasized here that the degree of chain orientation in the nanofiber is increased by increasing the rotating speed (see the following discussion on molecular orientation in electrospun POM nanofiber). The important point here is that even without applying any such tensile force to the fibers; we can get nanofibers with highly developed ECC morphology. This is a quite important finding in the technical development of the electrospinning method.

Molecular Orientation in Electrospun POM Nanofiber. Figure 3 shows the polarized FTIR spectra of electrospun POM nanofibers, which were collected with the rotating disk collector under a take-up velocity of 0, 630, and 1890 m/min. A small portion of the as-spun POM nanofiber is picked up, with special care to avoid any force and tension disturbing or destroying the morphology during sample preparation. Figure 3a shows

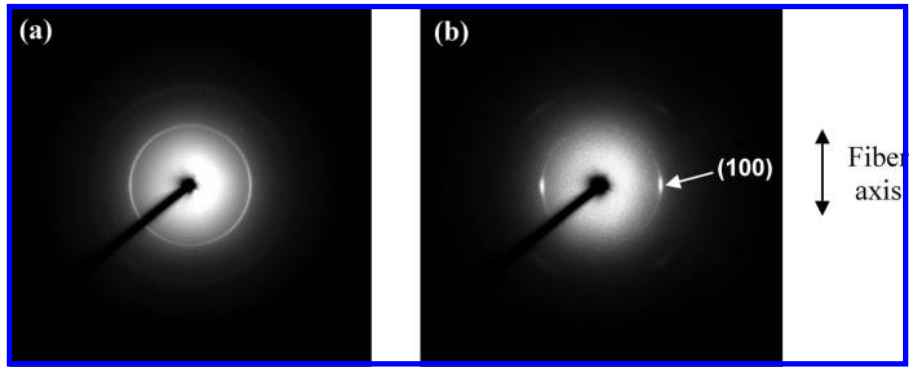

Figure 4. Two dimensional (2D) WAXD patterns for the 100 reflection of aligned POM nanofiber at (a) 630 m/min and (b) 1890 m/min.

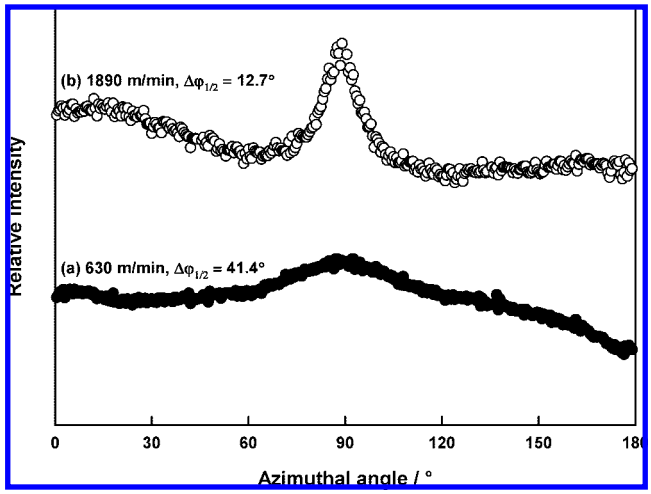

Figure 5. Azimuthal-scan profiles for the 100 reflection for aligned POM nanofibers with a take-up velocity of (a) 630 m/min and (b) 1890 m/min.

that parallel components of the IR peaks observed at $A_2(4)$ and $A_2(3) + E_1(7)$ bands are significantly higher than those observed for the perpendicular components. This implies that the electrospinning process originally induces the molecular orientation to be parallel to the fiber axis.

A polymer solution is believed to experience two kinds of force during electrospinning; one is a shear force when it flows through the capillary (needle) at a very high rate and the other is a Columbic force when the jet is elongated and accelerated by the applied high electric field. Both the shear force and the Columbic force possibly initiate synergistically the orientation of the polymer chain. Here, it is expected that an increase in mechanical force during the disk rotation will initiate the increase in molecular orientation of the polymer chain. As we expected, when the take-up velocity of the collector was increased from 0 m/min to 630 m/min, and further increased to 1890 m/min, the parallel IR bands of $A_2(4)$ and $A_2(3)+E_1(7)$ increase remarkably, indicating the better alignment of the polymer chain (Figure 3b and 3c). It is important to notice that the frequency position of the $A_2(4)$ band corresponding to the ECC morphology is shifted from 900 cm^{-1} to 898 cm^{-1} and to 894 cm^{-1} as the take-up velocity of the rotating disk collector is increased from 0 to 630 and to 1890 m/min, respectively. This implies that an increase in the tensile stress applied to the fiber accelerates the ECC morphology with a significant defined structure.

To quantify the degree of uniaxial orientation exhibited by the POM molecules, the concept of a dichroic ratio was applied. Dichroic ratio (R) can be calculated by using the formula $R = A_{//}/A_{\perp}$, where $A_{//}$ is infrared absorbance of the parallel component, and $A_{\perp}$ is that of the perpendicular component. For a randomly oriented sample, R is equal to 1, and for a perfectly uniaxially oriented sample (all polymer chains are oriented along the fiber axis), R is equal to infinity. The dichroic ratios for the IR bands of the POM nanofibers are summarized in Table 2. The infrared peak observed at the $A_2(4)$ band ($\sim$900 cm^{-1}) corresponds to the ECC, whereas that observed at the $A_2(3)$ band ($\sim$1120 cm^{-1}) corresponds to the FCC. As the take-up velocity of the rotating disk collector increases, the ECC component is increased, whereas the FCC component is decreased. The FCC peak could not be observed at the highest take-up velocity (1890 m/min), resulting in the nonexistence

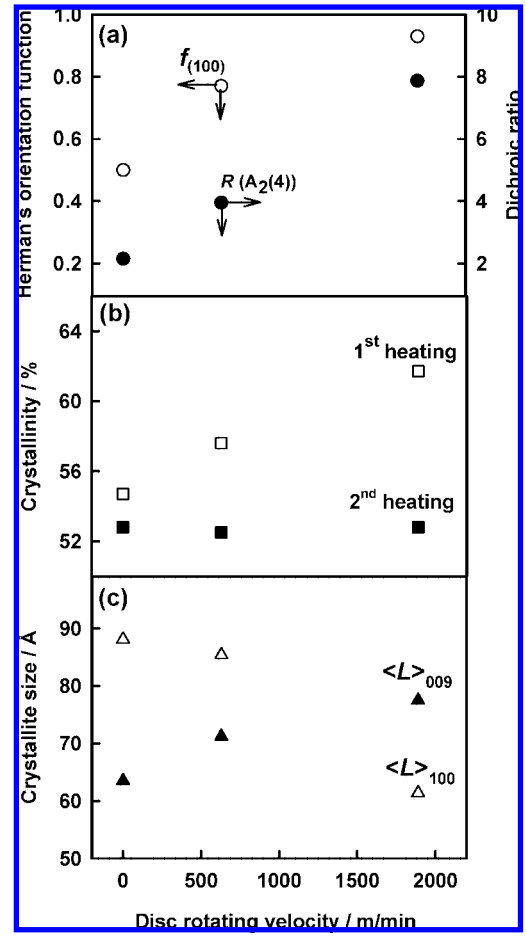

Figure 6. (a) Herman's orientation function (○) and dichroic ratio of $A_2(4)$ band at 900 cm^{-1} (●), (b) crystallinity estimated from the enthalpy of melt of the 1st heating (□) and 2nd heating (■), and (c) crystallite size estimated from 100 reflection (Δ) and 009 reflection (▲), as a function of take-up velocity of the rotating disk collector.

of R value. This implies that the polymer chains in the crystalline region can be stretched farther in the draw direction during the take-up process.

As the FTIR spectra clearly shows us that the disk rotating speed easily controls the ECC morphology, it is important to find clarification about the polymer chain orientation at the molecular level. Here, the molecular orientation in electrospun POM nanofibers was further investigated by 2D WAXD. Figure 4 shows the 2D WAXD patterns of the aligned POM nanofibers collected at a take-up velocity of 630 and 1890 m/min. By comparing these two patterns, it is clear that the disk rotating speed significantly enhances the orientation of the c-axis into the fiber direction. Comparison of the azimuthal profile of the two nanofibers obtained from the different disk rotating speeds clearly shows that the full width at half maximum (fwhm) of the fiber obtained from the disk rotating speed of 1890 m/min is significantly smaller than that observed at 630 m/min, suggesting lower degree of misorientation of the polymer chain along the fiber axis (Figure 5).

In order to identify the amount of misorientation of the nanofibril in the nanofiber, Herman's orientation function was applied. Figure 6a shows Herman's orientation function for our fibers. Herman's orientation function (f) is defined as:

$$f = \frac{3\langle \cos^2 \phi \rangle - 1}{2} \quad (1)$$

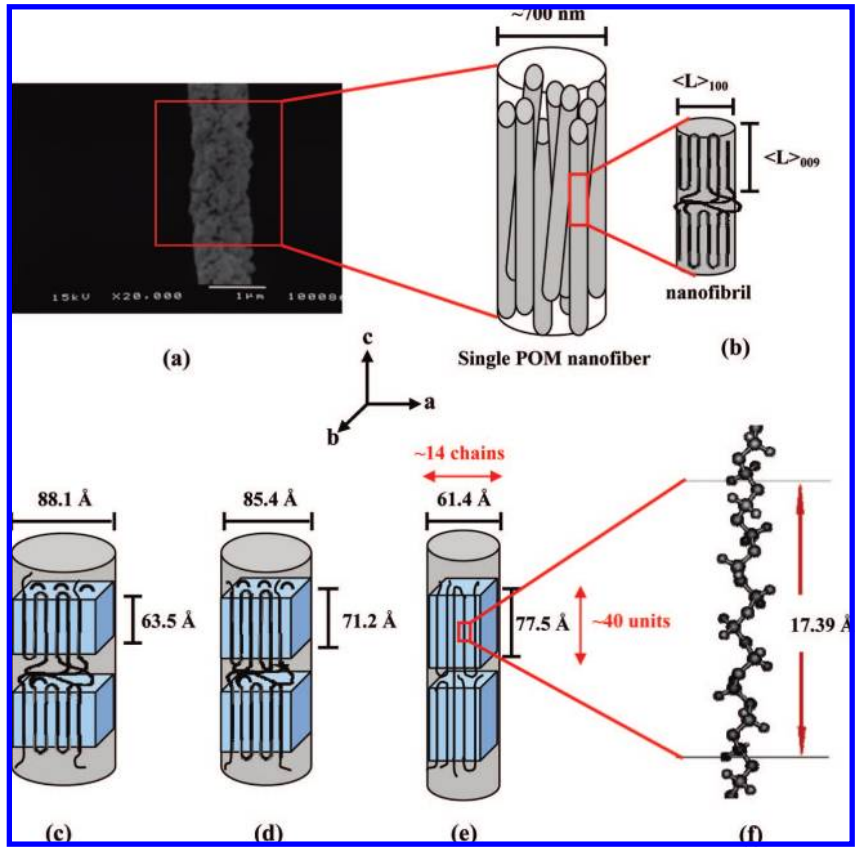

Figure 7. (a) SEM micrograph of a single POM nanofiber collected at 630 m/min; (b) schematic representations of nanofibril in a single POM nanofiber; (c−e) schematic representations of the crystal orientation of (c) POM at 0 m/min, (d) POM at 630 m/min, and (e) POM at 1890 m/min; and (f) crystal conformation of the (9/5) helical structure of the POM chain.

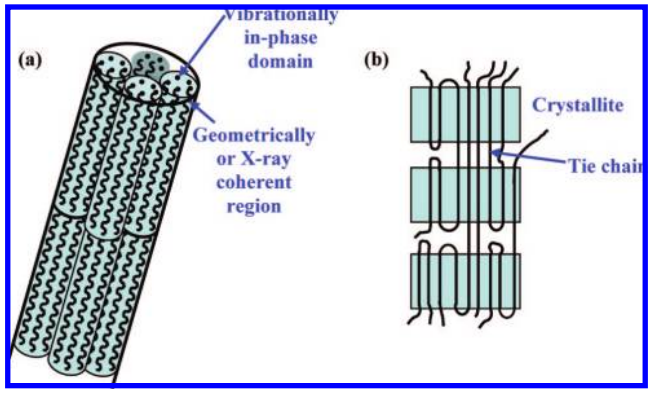

Figure 8. Schematic of (a) vibrationally in-phase domain and geometrically coherent region and (b) existence of tie chains between the neighboring crystallites.

where $\cos^2 \varphi$ represents a square averaged cosine of angle φ between the fiber axis and the crystallographic axis. The value of f is 1 when the polymer chains align perfectly parallel to the fiber axis, and -0.5 when the polymer chains align perfectly perpendicular to the fiber axis. When f is zero, it means there is random orientation. In our case, the calculation of f was simplified by simply calculating the misorientation appearing in the azimuthal scan, as shown in Figure 5. The value of f can then be calculated by the following equation:

$$f = \frac{180° - \Delta\phi_{1/2}}{180°} \qquad (2)$$

where $\Delta\varphi_{1/2}$ represents the fwhm of the azimuthally scanned peak (Figure 5). Figure 6a shows the calculated f, and it is clear that the orientation function increases as the take-up velocity of the rotating disk collector is increased. Especially, the nanofiber obtained at 1890 m/min gives $f = 0.93$, which is very close to 1, indicating that the polymer chains are oriented and are almost parallel to the fiber axis. It should be noted that the dichroic ratio (R) is also increased with the same trend as the Herman's orientation function.

Degree of Crystallinity and Crystallite Size. Table 2 also shows the enthalpy of melt of the as-spun and aligned POM nanofibers. In our case, the enthalpy of melt observed in the first heating (ΔH_m, first heating) refers to the degree of crystallinity initiated by the electrospinning process. On the other hand, the ΔH_m observed in the second heating refers to the degree of crystallinity after slowly cooling from the melt. The ΔH_m observed in the first heating increases gradually as the rotating speed is increased, implying an increase in crystallinity. Besides, it is significantly higher than that observed in the second heating. The degree of crystallinity was calculated on the basis of the melting enthalpy of a 100% crystalline POM sample which is 317.9 J/g as reported by Iguchi et al.[31] Figure 6b clearly shows the change in crystallinity as an effect of the electrospinning process with various rotating disk collectors, which confirms how the electrospinning process induces the crystallization of POM. Because the ΔH_m and the crystallinity obtained from the second heating is rather stable and lower than those of the first heating, we speculate that the orientation via fiber stretching during the spinning and collecting on the rotating disk reverts back to the average packing via thermal treatment.

(31) Iguchi, M. *Makromol. Chem.* **1976**, *177*, 549–566.

Figure 6c shows the change in crystallite size estimated from Scherrer's equation for the 100 and 009 reflections. As the take-up velocity of the rotating disk collector increases from 0 m/min to 630 m/min and to 1890 m/min, the $\langle L\rangle_{100}$ decreases from 88.1 Å to 85.4 Å and to 61.4 Å, respectively, whereas the $\langle L\rangle_{009}$ is simultaneously increased from 63.5 Å to 71.2 Å and to 77.5 Å. At this point, we may say the following: (i) the electrospinning method gives highly oriented ECC crystals with relatively high crystallinity even without any additional tension via the rotating disk, and (ii) by applying the tensile force during the disk rotation, the degree of orientation and the crystallinity are enhanced remarkably. At the same time, the crystallite size along the fiber direction is increased, while that in the lateral direction $<L>_{100}$ is decreased gradually.

Structure of POM Nanofiber. Considering the overall results, the detailed structure of the POM nanofiber is speculated with the schematic shown in Figure 7. Tadokoro et al. reported the crystal conformation of the (9/5) helical structure in the fiber period of 17.39 Å.[16] In the case of the electrospun POM nanofiber with a disk rotation at 1890 m/min, the $\langle L\rangle_{009}$ for 77.5 Å and $\langle L\rangle_{100}$ for 61.4 Å led us to a schematic nanofiber with about 40 monomeric units and a bundle of 14 chains arranged along the chain axis in an X-ray coherent domain.

According to Kobayashi et al., the *R*/*H* ratio of the crystallite governs the vibrational frequency of the infrared A_2 bands.[19] For example, the $\langle L\rangle_{100}/\langle L\rangle_{009}$ gives a value of 0.8 for the nanofiber obtained by a 1890 m/min rotating speed, which should predict the peak position of the A_2 band closer to FCC. This is inconsistent with the actually observed infrared spectral profile, which corresponds to the almost perfect ECC morphology. We speculate this situation in the following way: The infrared-active vibrational mode comes from the aggregation of groups vibrating in-phase. This can be applied for both the chain direction and the lateral direction. The X-ray diffraction occurs from the domain, which should consist of the positionally regular array of the groups. The coherent (or in-phase) size of the "static" and "vibrating" units might be different in some senses. In a single nanofiber, the vibrationally matched domains are aggregated to form a geometrically coherent region, as illustrated in Figure 8a. Another possibility is the existence of so-called tie chains between the neighboring crystallites, as proposed by Hama et al.[23] The extended chains can pass through the neighboring crystallites and form small sized bundles (Figure 8b). These bundles have a smaller *R*/*H* ratio because $H \gg R$. These bundles do not contribute to the X-ray diffraction positively but remarkably affect the infrared spectral profile. A more detailed investigation of the relation between the *R*/*H* ratio estimated by the IR data and the crystallite size by X-ray data is needed.

Conclusion

Generally, POM is a highly crystalline polymer with the folded chain crystal (FCC) structure. The work showed that the extended chain crystal (ECC) could be easily achieved by electrospinning process combined with the take-up technique. By controlling the electrical voltage and the take-up velocity of the rotating disk collector, the morphology is interchangeable between the ECC and FCC. Molecular orientation parallel to the fiber axis was observed in both isotropic and anisotropic POM nanofibers. The high rotating disk velocity not only induced the ECC morphology but also enhanced the chain to be parallel to the fiber axis. On the basis of Herman's orientation and crystallite size estimated from the 100 and 009 reflections, it was clear that, at the highest rotating speed (1890 m/min), the nanofibrils aligned almost parallel to the fiber axis with a bundle of about 14 polymeric chains and around 40 monomeric units under the (9/5) helical structure. The present work demonstrated a new approach to control crystal morphology and molecular orientation by producing nanofibers via the electrospinning process with a rotating disk collector using polyoxymethylene as an example.

Acknowledgment. The authors are grateful for the financial support from Mitsubishi Gas Chemical Company, Japan, and Thai Polyacetal Co. Ltd., Thailand, especially Mr. Toshikazu Umemura, Mr. Yasushi Kousaka, and Mr. Daigo Nakaya. The authors are also appreciative of the grant from the University Mobility in Asia and the Pacific (UMAP) Program under the Ministry of Education, Thailand. One of the authors (T.K.) gratefully acknowledges the scholarship from the Petroleum and Petrochemical College, Chulalongkorn University.[5]

Supporting Information Available: Experimental section including material selection and procedures for electrospinning and characterizations. This material is available free of charge via the Internet at http://pubs.acs.org.

JA804185S